APPENDIX

Replication fork passage drives the asymmetric dynamics of a critical nucleoid-associated protein in *Caulobacter*

Rodrigo Arias-Cartin[1,2], Genevieve S. Dobihal[1,3,#], Manuel Campos[1,2,3], Ivan V. Surovtsev[1,2,3], Bradley Parry[1,2] and Christine Jacobs-Wagner*[1,2,3,4]

[1]Microbial Sciences Institute, Yale University, West Haven, CT 06516, USA
[2]Department of Molecular, Cellular, and Developmental Biology, Yale University, New Haven, CT 06520, USA
[3]Howard Hughes Medical Institute, Yale University, New Haven, CT 06520, USA
[4]Department of Microbial Pathogenesis, Yale Medical School, Yale University, New Haven, CT 06520, USA
*Corresponding author
[#]Present address: Department of Microbiology and Immunology, Harvard Medical School, Boston, MA 02115, USA

Table of contents

Appendix Figure legends

Appendix Figure S1. Loss of SMC or HU function does not affect cell morphology or growth in *C. crescentus*.

A. Strains harboring in-frame deletions of Δ*smc*::km (strain ML2118) or a double deletion of *Δhup1*::sp and *Δhup2*::oxy that encode HU subunits (strain ML2120) were grown to exponential phase in M2G minimal medium prior to staining with DAPI to visualize the chromosome. Yellow lines show the cell contours detected with Oufti from the corresponding phase-contrast image. Scale = 2 µm

B. Cell length distributions of the Δ*hup1*Δ*hup2* and Δ*smc* deletion strains when grown under the indicated conditions. For each condition, at least 1275 cells were analyzed.

C. Doubling times based on OD_{660nm} measurements by a microplate reader for strains WT (CB15N), Δ*gapR::oxy gapR-Venus* (CJW5777), Δ*smc* and Δ*hup1*Δ*hup2.*

D. Phase-contrast images showing that WT cells and cells expressing GapR-Venus at *xylX* locus as the only copy (CJW5777) have the same morphology. Scale = 2 µm.

Appendix Figure S2. GapR binds DNA in *E. coli*

A. Colocalization of the nucleoid and *C. crescentus* GapR in an *E. coli* cell expressing GapR-sfGFP (strain CJW5794). Expression of GapR-sfGFP was induced with 0.02% arabinose for 2 h in M9Glycerol medium, followed by DAPI staining. Scale = 1 µm.

B. Fluorescence intensity profiles of GapR-sfGFP and DAPI signals along the length of the cell shown in panel A.

C. SDS-PAGE analysis of purified 6His-GapR protein (~10 µg) stained with Coomassie.

Appendix Figure S3. Deletion of *CCNA_03907* is not associated with morphological or growth defects in *C. crescentus*.

A. Chromosomal location of *CCNA_03907*.

B. Phase-contrast images showing the morphology of cells deleted for CCNA_03907 (CJW5816), the gene directly downstream of *gapR*. For imaging, strain CJW5816 harboring an in-frame deletion of *CCNA_03907*::Ω was grown to exponential phase in M2G minimal medium or PYE rich medium at 25 or 30˚C. Scale = 2 µm.

C. Cell length distributions of *CCNA_03907*::Ω deletion strain when grown under indicated conditions. For each condition, at least 1187 cells were analyzed.

D. Doubling times based on OD_{660nm} measurements by a microplate reader. The growth conditions correspond to those in panel B.

Appendix Figure S4. Distribution of cells with and without DnaN-mCherry foci in *C. crescentus*.

A. Histogram of cell length for CJW5800 cells exhibiting 0, 1 or 2 DnaN-mCherry foci in strain CJW5800 (n = 8358 cells). The integral of each curve is 1. See Computer Code EV1A information for details of foci detection algorithm.

B. Same as A but relative to the fraction of the population (number of cells with 0 spot = 2103, 1 spot = 4683, 2 spots = 1476 and >2 spots = 96).

Appendix Figure S5. Correlated dynamics of GapR and DnaN localization during the cell cycle.

Kymographs showing the localization of GapR-Venus and DnaN-CFP over time in 5 different cells (strain CJW5932) following synchrony. Cellular coordinates were oriented using the DnaN-CFP bright focus as an old-pole marker.

Appendix FigureS6. HU2-mCherry and DnaN dynamics are independent during the cell cycle.

Kymographs showing the localization of HU2-mCherry and DnaN-CFP over time in 5 different cells (strain CJW5963) following synchrony. Cellular coordinates were oriented using the DnaN-CFP bright focus as an old-pole marker.

Appendix Figure S7. Cell cycle dynamics of GapR localization are not caused by changes in CcrM-dependent methylation

A. Demograph showing the cell cycle localization of GapR-Venus in an asynchronous population (n = 2700 cells) of a strain (CJW5825) constitutively producing CcrM. The fluorescence profile across cell was normalized by cell length for each cell. Cells were sorted by increasing cell length, and cell coordinates were oriented using TipN-CFP as a new-pole marker.

B. Kymographs showing the spatial distribution of Red-Venus and DnaN-CFP over time in 4 different CJW5775 cells constitutively producing CcrM. Time-lapse microscopy started right after synchrony. Cell coordinates were oriented using DnaN-CFP bright focus as an old-pole marker.

Appendix Figure S8. GapR forms long-lived complexes with DNA that are disrupted by replisome progression

Kymographs of 3 different FtsZ-depleted cells (CJW5808) expressing GapR-Venus and DnaN-CFP. FtsZ depletion was initiated after synchronization by allowing cells to resume cell cycle progression without xylose (*ftsZ* expression inducer).

Appendix Figure S9. Simulations showing the effect of spontaneous dissociation vs. no dissociation from DNA on the localization profile of a DNA-binding protein

A. Distribution of a fluorescently-labeled DNA-binding protein in a simulation of the replisome-dependent model with spontaneous protein dissociation from the DNA. The simulation started with a random distribution and considered a spontaneous dissociation from the DNA with a characteristic time of τ = 1 min. Protein re-association with the DNA occurred with a uniform probability along the DNA, thereby homogenizing protein distribution over time, as shown in a kymograph.

B. Same random distribution at t = 0 and simulated as in A, except for no spontaneous dissociation. Because of the lack of dissociation from the DNA, the initial stochastic distribution of the DNA-binding protein is maintained over time. As a result, any stochastic accumulations present at t = 0 is retained, producing horizontal streaks of fluorescent signal in kymographs.

Appendix Figure S10. The asymmetric distribution of GapR over the chromosome is maintained over replication cycles in the replisome-eviction model.

Simulated profile of GapR in G1 phase for each cycle of DNA replication. Simulations start with a uniform distribution of GapR along the chromosome (Replication cycle 1). After 9 replication cycles, the distribution of GapR in the following G1 phase (10^{th} convolved) was convolved with a point spread function corresponding to our optical set-up.

Appendix Figure S11. Comparison between the GapR ChIP-seq coverage and the replisome-eviction model over the chromosome in an asynchronous population

The chromosomal profile of the GapR ChIP-seq data from an asynchronous experiment was overlayed with the model prediction (black line = simulated profile). For the ChIP data, the coverage reads were normalized to the total area of the distribution. Calculation of the simulated profile was based on the cell age distribution and the fraction of cells ongoing DNA replication (S phase) in an asynchronous population (n = 8358 cells, CJW5800 cells) expressing DnaN-CFP. For details, see Appendix Supplementary Methods section.

Appendix Figure S12. Spontaneous dissociation of GapR from the DNA with a characteristic time of τ_{off} = 100 min does not affect the binding asymmetry of GapR

We generated the same simulations, plots and kymographs as in Fig 8, except that here we used a modified replisome-dependent model in which GapR spontaneously dissociates from the DNA with a characteristic time τ_{off} = 100 min.

A. One-dimensional simulation of the replisome-eviction model showing the evolution of GapR distribution on replicated and unreplicated DNA during replisome progression. In the model, GapR is synthesized throughout the cell cycle such that its amount (1,000 molecules) has doubled by the end of the cell cycle. At t = 0 (in cell cycle unit), GapR binding along the chromosome is uniform. We assume that replication starts at t = 0.3 and ends at t = 0.9. The replisome moves at a constant speed from *ori* to *ter*, and leaves behind 2 copies of the replicated DNA region (sister chromatids). When the replisome encounters GapR, the replisome displaces GapR from the DNA. In addition, GapR spontaneously dissociates from the DNA with a characteristic time τ_{off} = 100 min. The displaced and dissociated GapR is then randomly redistributed, with uniform probability over the two replicated regions and the unreplicated region.

B. Same as in A, but starting with the GapR distribution at t = 1 in panel A to show the effect of a second round of replisome progression on GapR distribution on replicated and unreplicated DNA.

C. Kymograph of simulated GapR distribution over cell cycle time in wild-type cells. The green dashed line indicates replisome progression. GapR distribution between t= 0 and t = 0.2 is the same as between t = 0.2 and t = 0.3.

D. Same as C but after convolution of the GapR signal with an idealized Gaussian PSF with a standard deviation of our optical set-up (0.065 in relative cell-length units).

A

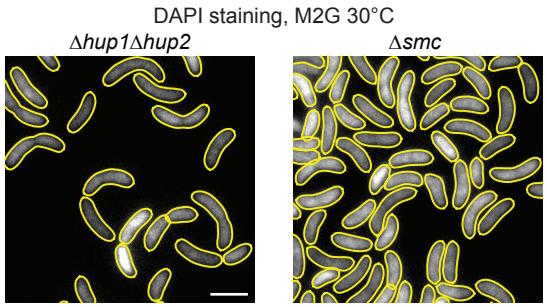

B

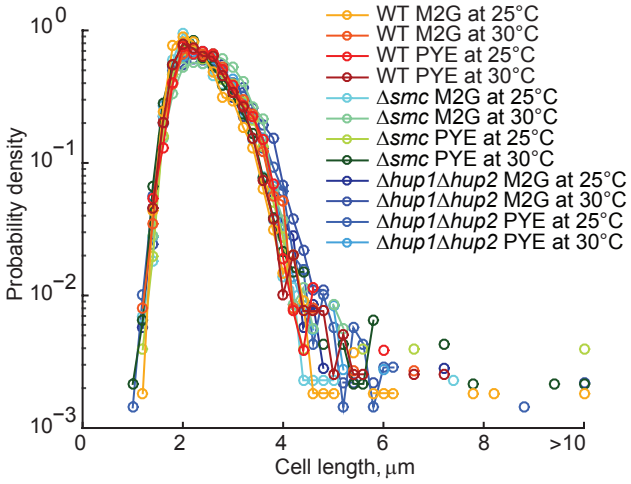

C

Strain description	Growth medium	Doubling time, min	
		30°C	25°C
WT	M2G	117 ± 1	168 ± 2
Δ*gapR gapR-venus*	M2G	120 ± 1	167 ± 1
Δ*smc*	M2G	108 ± 1	170 ± 7
Δ*hup1*Δ*hup2*	M2G	120 ± 1	165 ± 2
WT	PYE	99 ± 1	134 ± 4
Δ*gapR gapR-venus*	PYE	100 ± 1	125 ± 5
Δ*smc*	PYE	91 ± 1	131 ± 1
Δ*hup1*Δ*hup2*	PYE	99 ± 1	139 ± 1

D

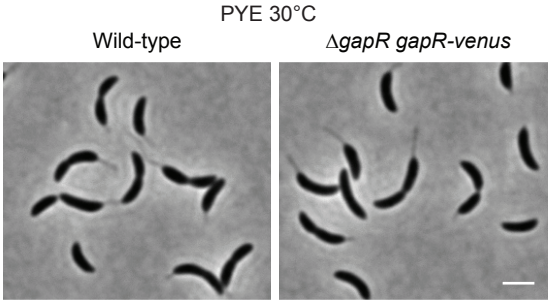

Figure S1

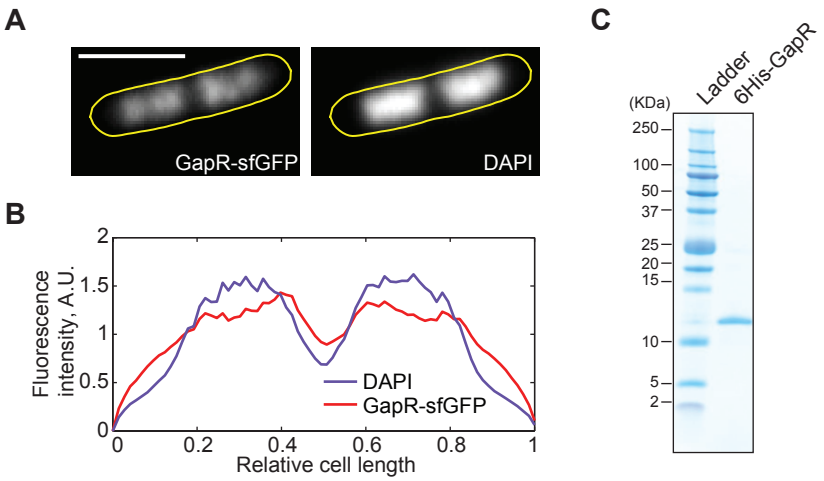
A
GapR-sfGFP
DAPI
B
Fluorescence intensity, A.U.
2
1.5
1
0.5
0
0
0.2
0.4
0.6
0.8
1
Relative cell length
DAPI
GapR-sfGFP
C
Ladder
6His-GapR
(KDa)
250
100
50
37
25
20
15
10
5
2

Figure S2

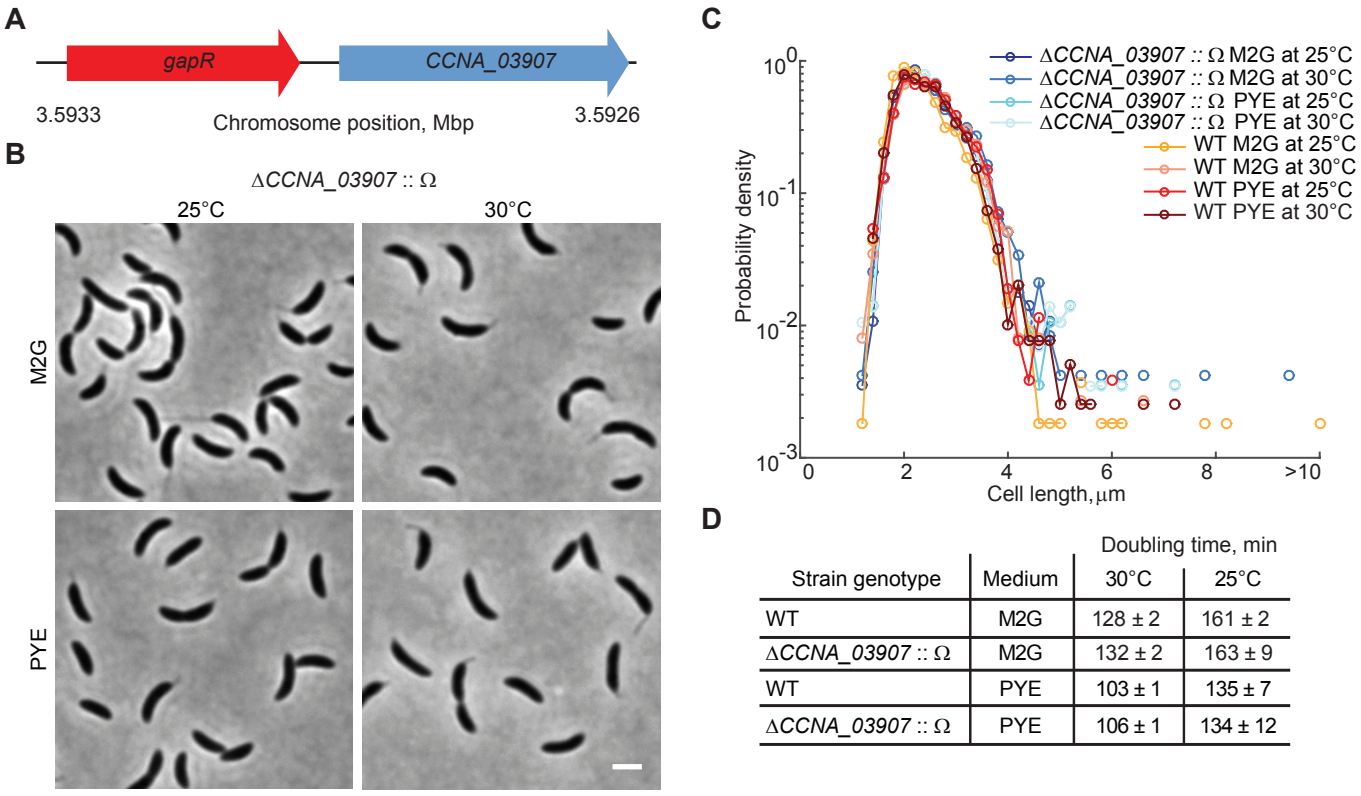

Strain genotype	Medium	Doubling time, min 30°C	25°C
WT	M2G	128 ± 2	161 ± 2
ΔCCNA_03907 :: Ω	M2G	132 ± 2	163 ± 9
WT	PYE	103 ± 1	135 ± 7
ΔCCNA_03907 :: Ω	PYE	106 ± 1	134 ± 12

Figure S3

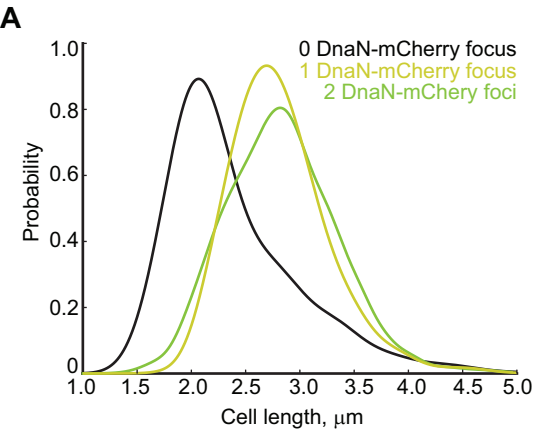
A
0 DnaN-mCherry focus
1 DnaN-mCherry focus
2 DnaN-mChery foci
Probability
1.0
0.8
0.6
0.4
0.2
0
1.0
1.5
2.0
2.5
3.0
3.5
4.0
4.5
5.0
Cell length, μm

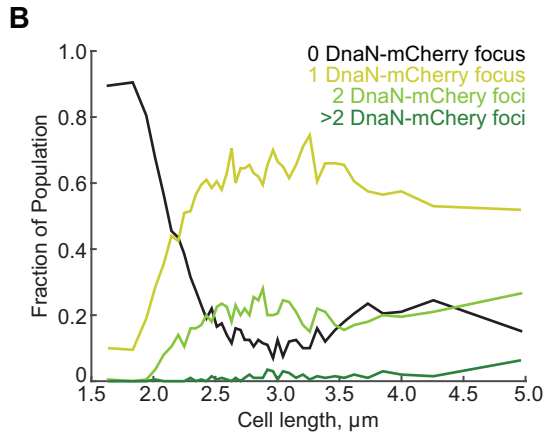
B
0 DnaN-mCherry focus
1 DnaN-mCherry focus
2 DnaN-mChery foci
>2 DnaN-mCherry foci
Fraction of Population
1.0
0.8
0.6
0.4
0.2
0
1.5
2.0
2.5
3.0
3.5
4.0
4.5
5.0
Cell length, μm

Figure S4

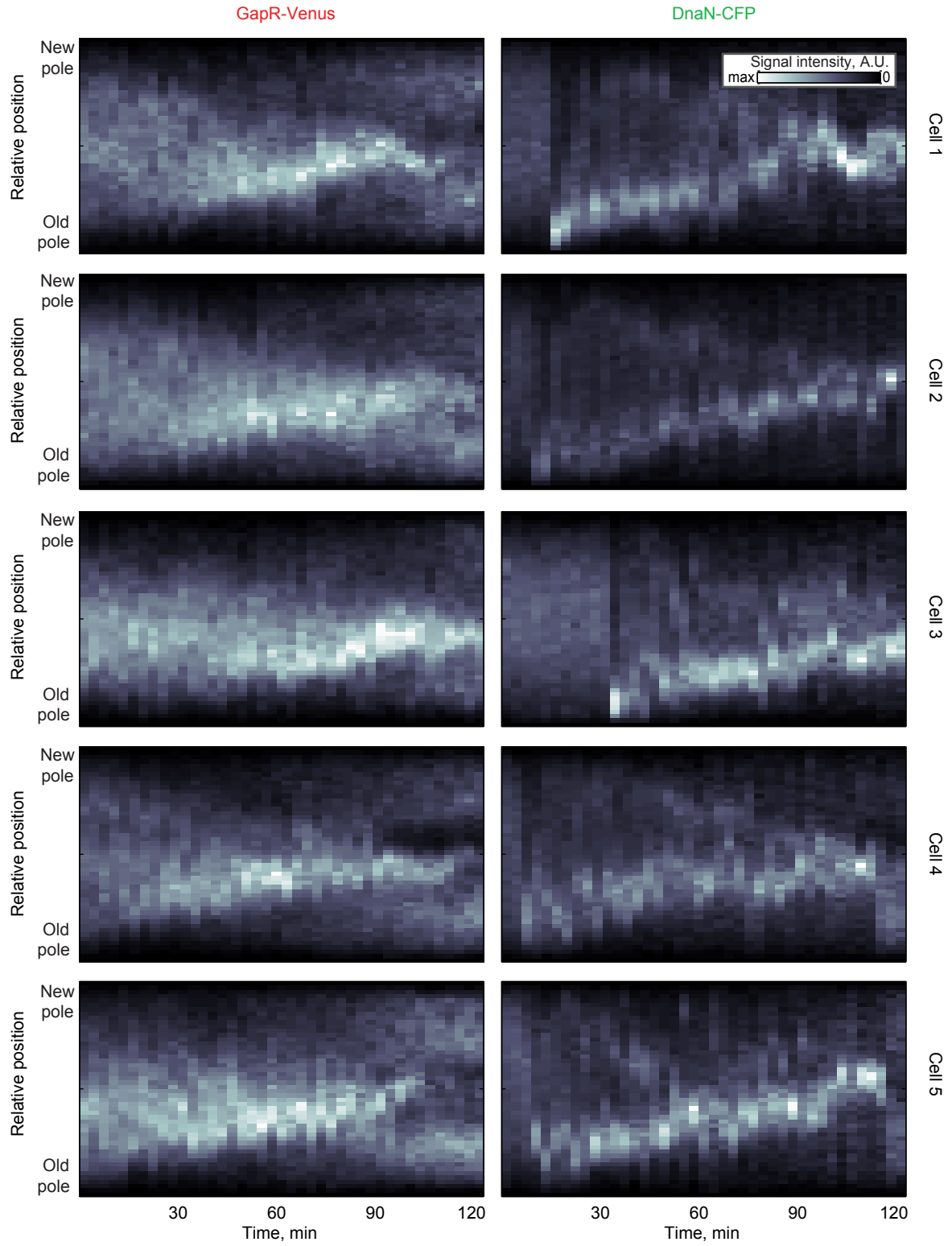
GapR-Venus
DnaN-CFP
Signal intensity, A.U.
max
0
New pole
Old pole
Relative position
Cell 1
Cell 2
Cell 3
Cell 4
Cell 5
30
60
90
120
Time, min

Figure S5

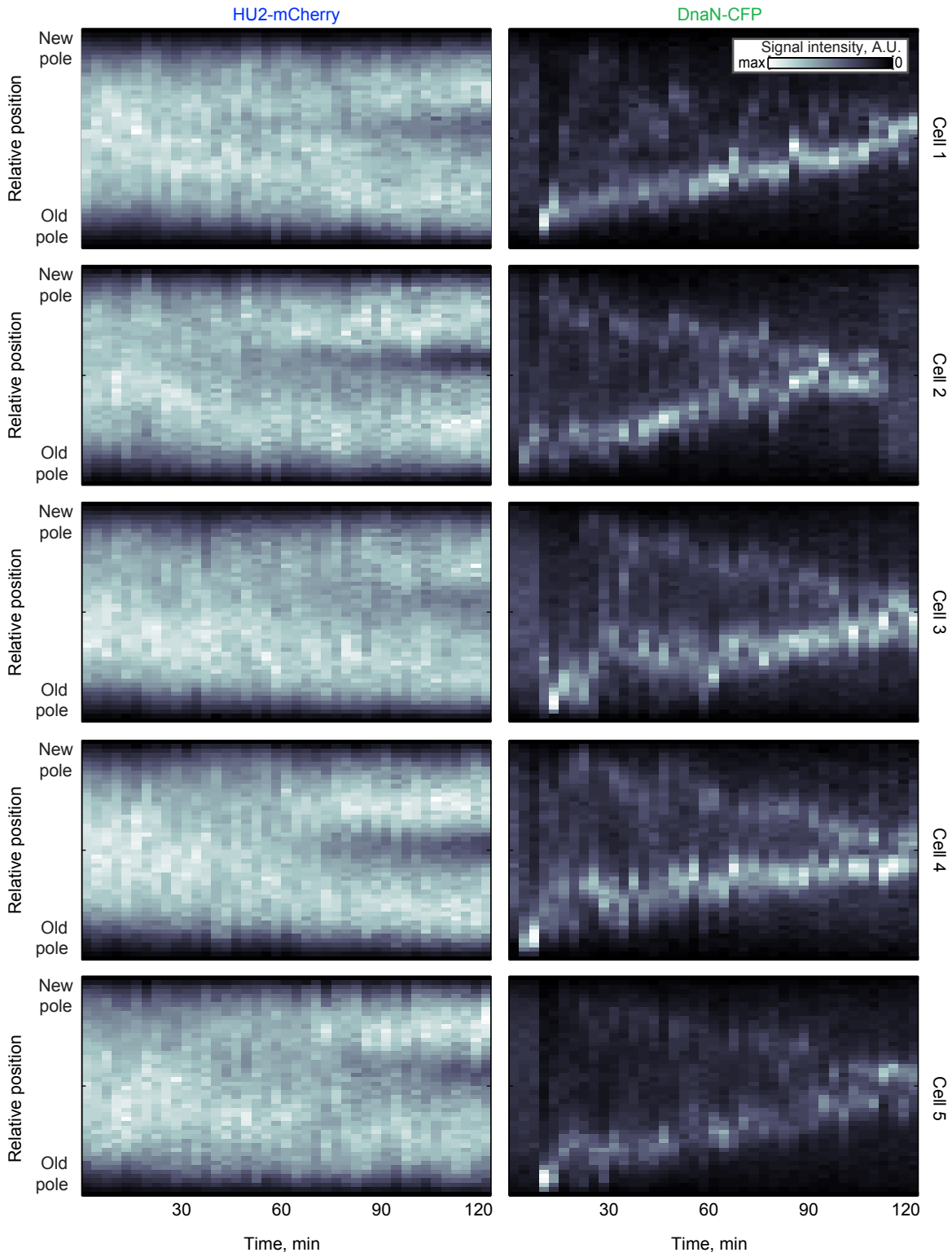
HU2-mCherry
DnaN-CFP
Signal intensity, A.U.
max
0
New pole
Old pole
Relative position
Cell 1
Cell 2
Cell 3
Cell 4
Cell 5
30
60
90
120
Time, min

Figure S6

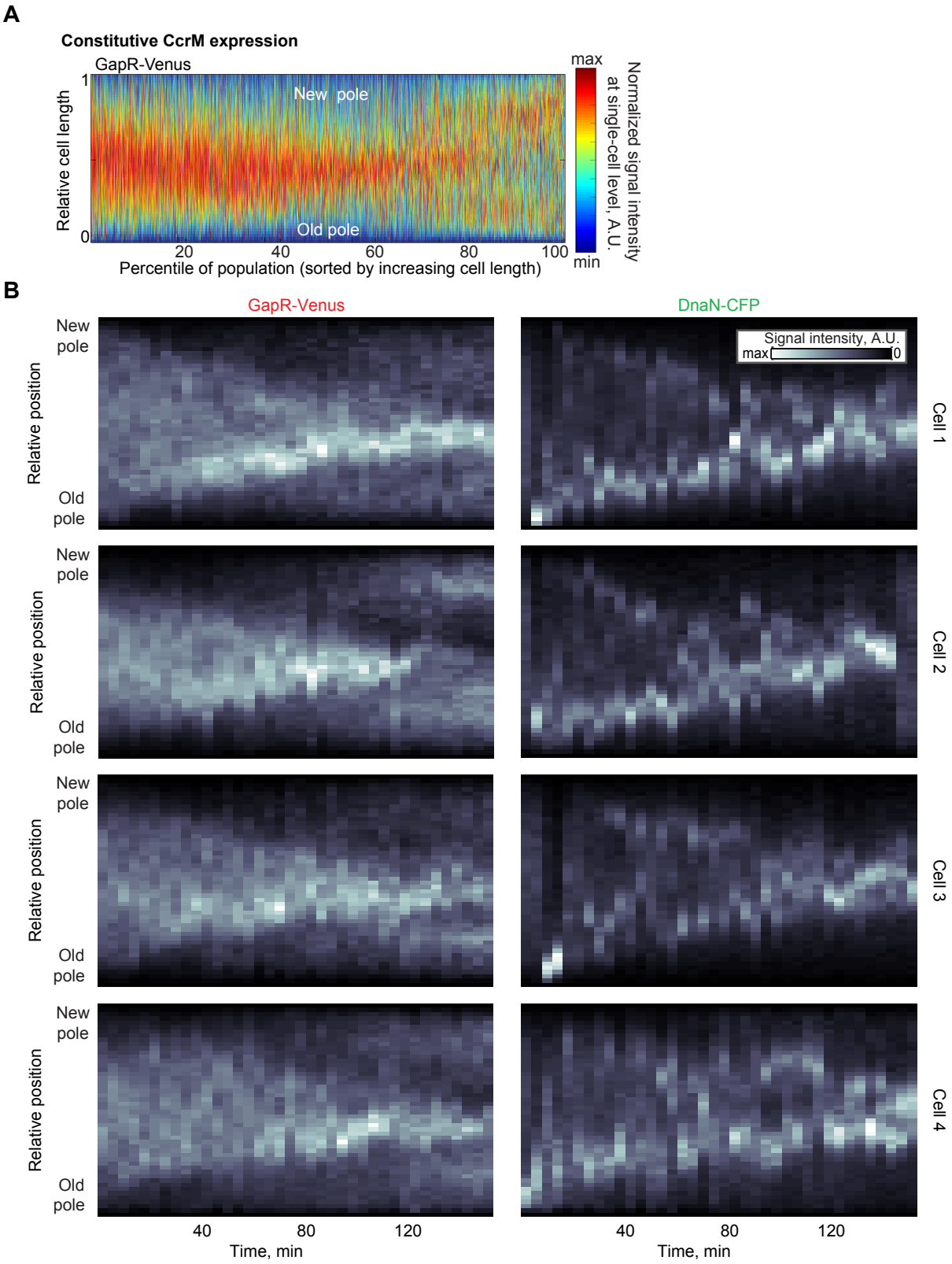
A
Constitutive CcrM expression
GapR-Venus
New pole
Old pole
Relative cell length
1
0
20
40
60
80
100
Percentile of population (sorted by increasing cell length)
max
min
Normalized signal intensity at single-cell level, A.U.
B
GapR-Venus
DnaN-CFP
Signal intensity, A.U.
max
0
Relative position
New pole
Old pole
Cell 1
Cell 2
Cell 3
Cell 4
40
80
120
Time, min

Figure S7

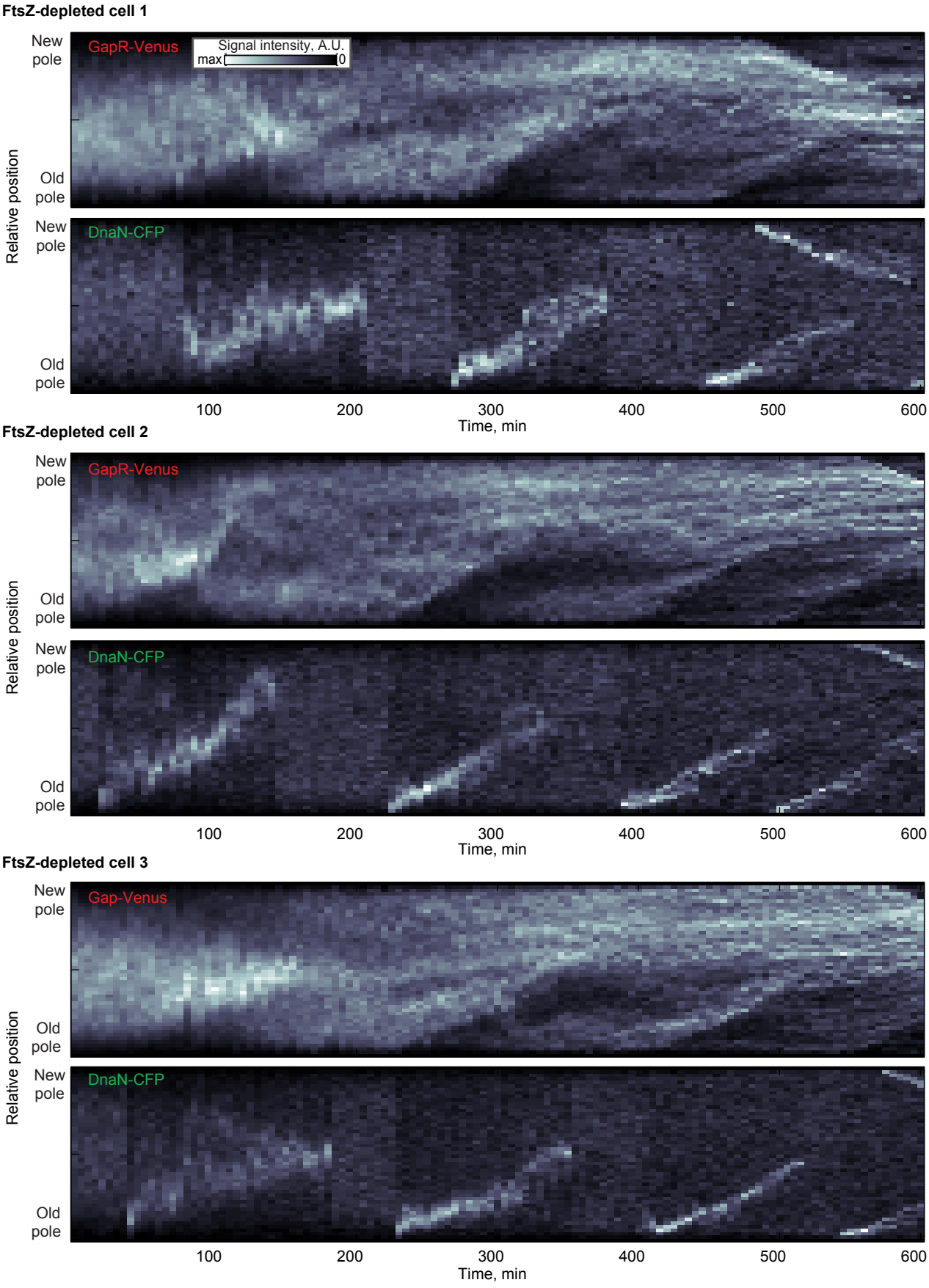
FtsZ-depleted cell 1
New pole
GapR-Venus
Signal intensity, A.U.
max
0
Old pole
Relative position
New pole
DnaN-CFP
Old pole
100
200
300
400
500
600
Time, min
FtsZ-depleted cell 2
New pole
GapR-Venus
Old pole
Relative position
New pole
DnaN-CFP
Old pole
100
200
300
400
500
600
Time, min
FtsZ-depleted cell 3
New pole
Gap-Venus
Old pole
Relative position
New pole
DnaN-CFP
Old pole
100
200
300
400
500
600
Time, min

Figure S8

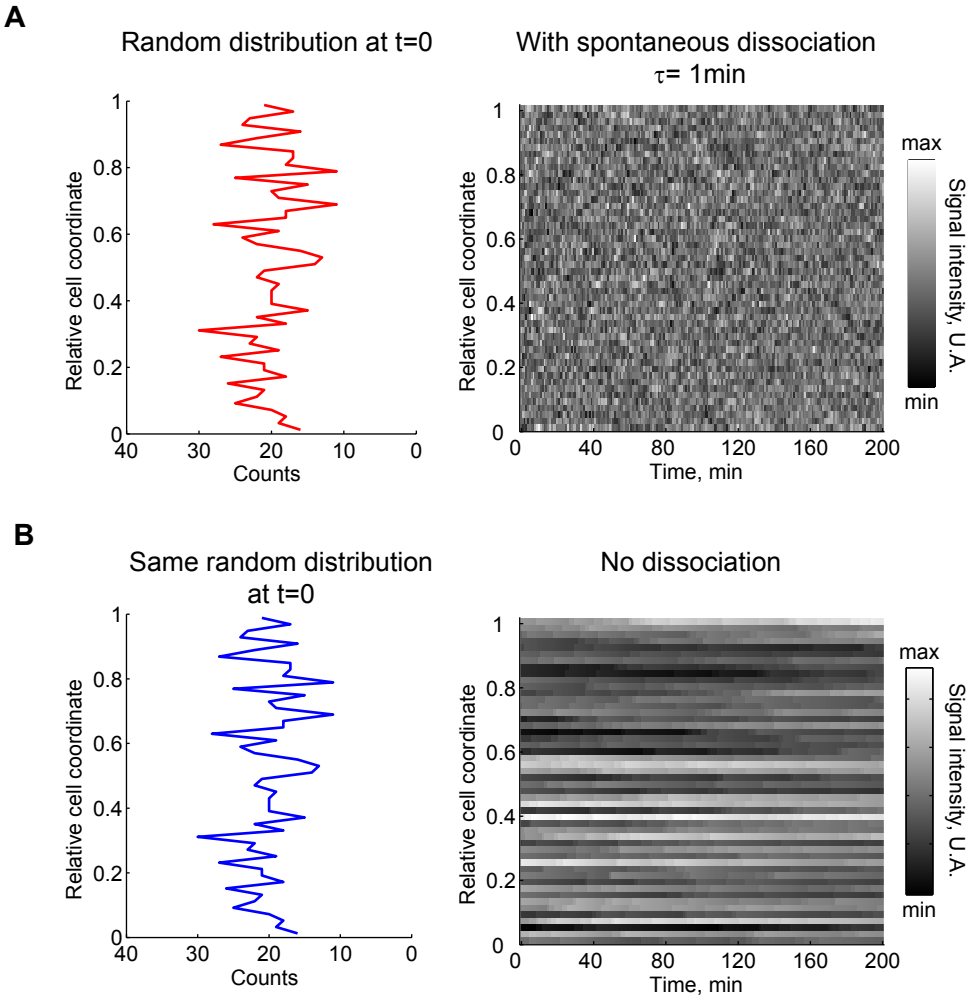
A
Random distribution at t=0
With spontaneous dissociation
τ= 1min
Relative cell coordinate
Counts
Time, min
max
min
Signal intensity, U.A.
B
Same random distribution
at t=0
No dissociation

Figure S9

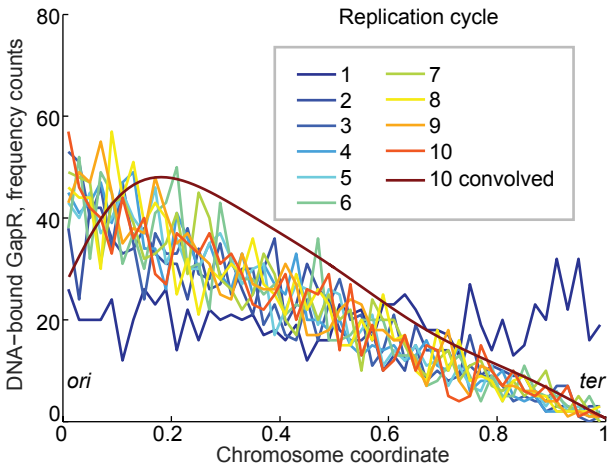
Replication cycle
1
2
3
4
5
6
7
8
9
10
10 convolved
DNA−bound GapR, frequency counts
80
60
40
20
0
ori
ter
0
0.2
0.4
0.6
0.8
1
Chromosome coordinate

Figure S10

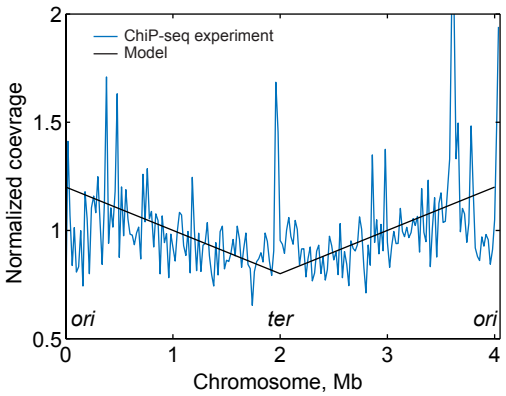
ChiP-seq experiment
Model
Normalized coevrage
2
1.5
1
0.5
ori
ter
ori
0
1
2
3
4
Chromosome, Mb

Figure S11

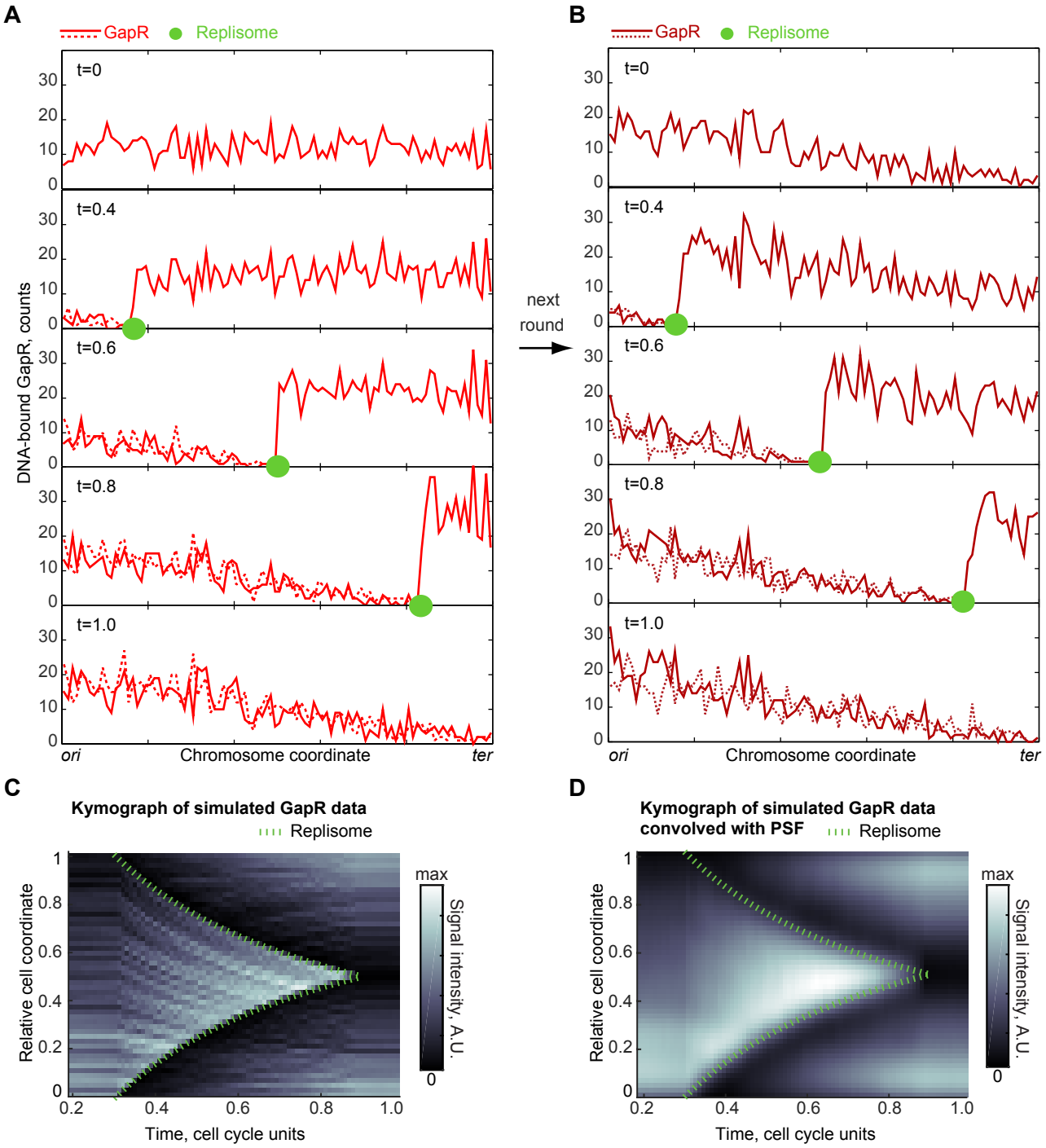
A
GapR
Replisome
t=0
t=0.4
t=0.6
t=0.8
t=1.0
DNA-bound GapR, counts
ori
Chromosome coordinate
ter
next
round
B
GapR
Replisome
t=0
t=0.4
t=0.6
t=0.8
t=1.0
ori
Chromosome coordinate
ter
C
Kymograph of simulated GapR data
Replisome
Relative cell coordinate
Time, cell cycle units
max
Signal intensity, A.U.
0
D
Kymograph of simulated GapR data
convolved with PSF
Replisome
Relative cell coordinate
Time, cell cycle units
max
Signal intensity, A.U.
0

Figure S12

Appendix Supplementary Methods

Media composition

LB medium: 10 g/L NaCl, 5 g/L yeast extract, 10 g/L tryptone

M9 supplemented medium: 6 g/L $Na_2HPO_4 \cdot 7H_2O$, 3 g/L KH_2PO_4, 0.5 g/L NaCl, 1 g/L NH_4Cl, 2 mM $MgSO_4$, 1 µg/L thiamine supplemented with 0.1% casamino acids and 0.2% glucose

PYE medium: 2 g/L bacto-peptone, 1 g/L yeast extract, 1 mM $MgSO_4$, 0.5 mM $CaCl_2$

M2G minimal medium: 0.87 g/L Na_2HPO_4, 0.54 g/L KH_2PO_4, 0.50 g/L NH_4Cl, 0.2% (w/v) glucose, 0.5 mM $MgSO_4$, 0.5 mM $CaCl_2$, 0.01 mM $FeSO_4$

Buffers composition

EMSA buffer: 10 mM Tris-HCl pH 7.6, 1 mM $MgCl_2$, 0.5 mM EDTA, 0.5 mM DTT, 50 mM NaCl, 4% glycerol and 0.5 mg/mL poly(dI-dC)•poly(dI-dC)

TBE buffer: 10.7878 g/L Tris base, 5.55 g/L boric acid, 744 g/L disodium EDTA•$2H_2O$ pH 8.3

Blocking buffer: TBS with 5% Non-fat milk and 0.05% Tween 20

Immunoblotting

Cultures of *C. crescentus* were grown up to OD_{660nm} ≈ 0.4 and synchronized as reported previously (Evinger and Agabian, 1977), and isolated swarmer cells were resuspended in pre-warmed M2G to an approximate OD_{660nm} ≈ 0.2. At 15 min intervals, OD_{660nm} measurements were recorded, and 1 mL samples were pelleted and frozen at -80°C until future use. For preparation of cell lysates, pellets were resuspended in 50 mM Tris-HCl, 2% SDS, and normalized by recorded OD_{660nm} measurements. Lysates were separated on an SDS polyacrylamide gel and proteins were transferred to a nitrocellulose membrane. The membrane was first incubated in Blocking buffer for 1 h (same buffer was used in following steps, unless stated otherwise) and probed with a 1:10,000 dilution of anti-CtrA (Quon et al., 1996) for another hour, and a 1:10,000 dilution of secondary anti-rabbit HRP (BioRad). The membrane was then stripped using 100 mM ß-mercaptoethanol, 2% SDS, 62.5 mM Tris-HCl, pH 6.7, and washed. Next, the membrane was probed with a 1:2,000 dilution of anti-MreB (Figge et al., 2004), and a 1:10,000 dilution of secondary anti-rabbit HRP (BioRad). The membrane was again stripped and probed for GapR-Venus using a 1:1,000 dilution of anti-GFP JL-8 Living Colors® Av Monoclonal Antibody (Clontech Laboratories, Mountain View, CA), and a 1:10,000 dilution of secondary anti-mouse HRP (BioRad). At each step after incubation with a secondary HRP antibody, the membrane was incubated with Amersham ECL Prime Western Blotting Detection

Reagent (GE Healthcare Bio-Sciences, Pittsburgh, PA) and signals were detected on a Kodak film (Carestream Health) or on an Amersham Imager 600 (GE Healthcare Bio-Sciences).

Protein purification

The recombinant plasmid for expression of His-tagged GapR was transformed into the *E. coli* strain BL21 (DE3), resulting in strain CJW5785. Cultures from a fresh transformation were grown in 0.5 L of M9 supplemented with 0.2% glycerol and 100 µg/mL kanamycin at 37°C until the culture reached an $OD_{660nm} \approx 0.4$ and then synthesis of His-GapR was induced with 0.5 mM IPTG at 25°C for 3 h. Cells were harvested by centrifugation (6,500 x *g*) and pellets were washed twice with 20 mM MOPS pH 7.2 buffer and frozen at -80°C. Pellets were resuspended in Buffer A (20 mM Tris-HCl, 400 mM NaCl, 10% glycerol pH 7.6) supplemented with 60 U DNAse I (Thermo Fisher Scientific, Waltham MA) and incubated at room temperature for 10 min. Cell wall was partially degraded using 7.5 kU Ready-Lyse Lysozyme (Epicenter Biotechnologies, Madison WI) and incubated at room temperature for 5 min. One tablet of Protease Inhibitor Cocktail (Roche, Basel Switzerland) was added and the mixture was further incubated at 37°C for 10 min. Cell disruption and DNA cleavage were achieved by sonication using a Digital Sonifier® S-250D with (Branson Sonic Power Co, Danbury CT) with the 1/8" microtip: output 45%, 11-13 cycles 20" ON/40" OFF on ice. Cell debris was removed by centrifugation at 100,000 x g for 1 h 30 min at 4°C. Further steps were performed using an ÄKTA™-FPLC system (GE Healthcare Life Sciences) equipped with a Monitor UPC-900 with fixed absorbance at 280 nm and using the manufacturer's chromatographic filtration devices. The cleared supernatant was injected into a 1 mL His-Trap HP™ Ni-sepharose column, previously equilibrated in Buffer A. A step-wise elution of the protein was performed with Buffer B (20mM Tris-HCl, 400 mM NaCl, 10% glycerol, 500 mM imidazole pH 7.6). After evaluation with Coomassie Blue staining on polyacrylamide gels, the His-GapR fractions with the highest purity were pooled and the NaCl concentration was reduced to ~10mM by dialysis against Buffer Aq (20 mM Tris-HCl, 10% glycerol pH 8.0) at 4°C for at least 4 h using a Slide-A-Lyzer™ cassette with MWCO = 10 kDa (Thermo Fisher Scientific). Higher purity was achieved by further purification using an anion-exchange MonoQ™ 5/50 GL chromatography column in a linear gradient from 50 mM to 1M NaCl generated by mixing Buffer Aq and Buffer Bq (20mM Tris-HCl, 10% glycerol, 1M NaCl pH 8.0). Protein purity was again evaluated by Coomassie Blue staining and DNA contamination was verified by ratio absorbance at 260/280nm in a Nanodrop device (Thermo Fisher Scientific) and ethidium bromide staining in an agarose gel. Fractions with no DNA and with highest purity (~98%) were pooled, concentrated using an Amicon Ultra-14

MWCO = 10 kDa (EMD Millipore, Darmstadt Germany) and dialyzed 1:1,000 overnight against Buffer Aq. Protein concentration was determined at this step with Pierce™ BCA Protein Assay Kit (Thermo Fisher Scientific). Removal of the polyHis-tag was achieved by digestion with Turbo TEV protease (Eton Bioscience Inc., San Diego CA) overnight at 16°C according to the manufacturer's recommendations. The cleavage efficiency was approximately 90–95%. The sample was dialyzed against buffer Bq overnight at 4°C, and stored in small aliquots at −80°C or kept at 4°C for immediate use.

Library preparation, sequencing and analysis for RNA-seq experiments

External RNA standard controls were performed by adding 1 µl of a 1:100 dilution of ERCC ExFold RNA Spike-In Mix (Thermo Fisher Scientific) per 1 µg of extracted RNA prior removal of rRNA. Library preparation and removals of rRNA were both achieved using the ScriptSeq Complete Kit Bacteria (Illumina®, San Diego CA) following the manufacturer's protocols. Libraries were sequenced using HiSeq2500 (1x50bp) to generate more than 10M reads per sample. The sequence data from each sample was aligned to the *C. crescentus* NA1000 reference genome CP001340.1 using STAR (Dobin et al., 2013). Gene quantification and differential gene expression analysis was performed using featureCounts (Liao et al., 2014) and DESeq2 (Love et al., 2014), respectively.

Library preparation and sequencing for Chromatin Immunoprecipitation (ChIP-seq) experiments

Library preparation and sequencing was performed by the Yale Center for Genome Analysis as follows: ~10 ng of immunoprecipitated DNA was evaluated with a 2100 Bioanalyzer (Agilent Technologies, Santa Clara CA) using a high sensitivity Quant-iT™ DNA Assay Kit (Thermo Fisher Scientific). ChIP-DNA was further purified using Ampure XP SPRI beads (Beckman Coulter Genomics). The DNA was then end-repaired, A-tailed, adapter ligated, and enriched with 10 PCR cycles. Indexed libraries that met the appropriate cut-offs were quantified by quantitative real-time PCR and insert size distribution was determined with the LabChip® GX (Perkin Elmer, Waltham, MA). Samples with a yield ≥0.5 ng/µl and ~300bp were used for sequencing. Subsequently, sample concentrations were normalized to 10 nM and loaded into Illumina Rapid or High-output flow cells (Illumina®, San Diego CA) at a concentration that yielded 150-250 million passing filter clusters per lane. Samples were sequenced using 75 bp single or paired-end sequencing on an Illumina HiSeq 2500 according to Illumina protocols. The 6 bp index was read during an additional sequencing read that automatically followed the

completion of read 1. A positive control (prepared bacteriophage Phi X library) provided by Illumina was spiked into every lane at a concentration of 0.3% to monitor sequencing quality in real time.

ChIP-seq data analysis

Reads obtained from sequencing were trimmed using the FastX Trimmer of the FastX-toolkit software package, and aligned to the *C. crescentus* NA1000 reference genome CP001340.1 using the BWA-MEM software (Li and Durbin, 2009). Statistically significant enriched genomic regions were determined with MACS2 (Zhang et al., 2008) with pairwise alignment files of total DNA before ChIP as "control" and immunoprecipitated GapR-Venus DNA as "treatment" for each sample. Peaks were detected with flags --extsize 147, --nomodel, and –gsize 4e6. We further used the genomeCoverageBed function from the bedtools suite (Quinlan and Hall, 2010) to determine the per-base coverage from the alignment files used for peak detection. The raw coverage numbers were normalized to number of millions of mapped reads. Downstream analysis was done using MATLAB software. Sequencing results are available under Gene Expression Omnibus (GEO) accession number, GSE85344. Circular schemes for normalized coverage reads were generated with R ("The Comprehensive R Archive Network," CRAN.), CIRCOS (Krzywinski et al., 2009) or MATLAB software with 10 kb sliding average window.

Motif discovery with MEME

One hundred nucleotide-long sequences centered on the ChIP-Seq peaks detected by MACS2 were fed into MEME (Machanick and Bailey, 2011). MEME was run locally via the Tmod Toolbox (Sun et al., 2010) with the following parameters: 1 moti to find, motif width set to 15, background Markov model of length 2 based on *C. crescentus* NA1000 genome sequence and allowing sites on both DNA strands (-revcomp set to TRUE). AT-rich motifs were found regardless of the value of the motif length parameter (value range tested: 10 to 30). We also tested the robustness of the ET-rich motif discovery by changing the length of the Markov model up to 4 and by thresholding the input sequences using the peak quality score returned by MACS2. In both cases, increasing the stringency (long Markov model and stringent q-value threshold) led to a similar motif.

Whole genome sequencing

Genomic DNA (gDNA) was extracted using a ChargeSwitch Kit® (Thermo Fisher Scientific) following the manufacturer's protocol from exponential (OD_{660nm} <0.275) cultures of wild-type

(NA1000) or a Δ*gapR*::oxy strain (CJW5747) grown in M2G or PYE media at 25°C. After elution, gDNA quality and concentration was assessed by measurement of the A260/A280 and A260/A230 ratios with a Nanodrop device (Thermo Fisher Scientific) and ethidium bromide staining in agarose gel. gDNA integrity and size was evaluated by running an Agilent Bioanalyzer gel prior to library preparation. Library preparation and sequencing was performed by the Yale Center for Genome Analysis as follows: ~500ng of gDNA with size 10-20 Kb was sheared using a Covaris E210 (Covaris®, Woburn, MA) and further purified using Ampure XP SPRI beads (Beckman Coulter Genomics). The DNA was then end-repaired, A-tailed, adapter ligated and enriched with 5 PCR cycles. Indexed libraries were that met appropriate cut-offs were quantified by quantitative real-time PCR and insert size distribution was determined with the LabChip® GX (Perkin Elmer, Waltham, MA). Samples with a yield of ≥0.5 ng/µl were used for sequencing. Subsequently, sample concentrations were normalized to 2 nM and loaded into High-output flow cells (Illumina®, San Diego CA) at a concentration that yields ~200 million passing filter clusters per lane. Samples were sequenced using 75 bp paired-end sequencing on an Illumina HiSeq 2500 according to Illumina protocols. The 6 bp index was read during an additional sequencing read that automatically followed the completion of read 1. A positive control (prepared bacteriophage Phi X library) provided by Illumina was spiked into every lane at a concentration of 0.3% to monitor sequencing quality in real time. Reads obtained from sequencing were trimmed and aligned to the *C. crescentus* NA1000 reference genome CP001340.1 using the Bowtie software (Li and Durbin, 2009). Downstream analysis was done with MATLAB software. Whole Genome sequencing results are available under Sequence Read Archive (SRA) with the ID: SRP081124.

Calculation of the organization factor

The organization factor measures how much entropy a probability distribution can gain before reaching its theoretical maximum entropy, which is given by the entropy of its corresponding uniform distribution. Signals went through several pre-processing steps before organization factor calculation. Oufti cellList signals of DnaN-CFP or DnaN-mCherry were oriented and computationally synchronized at the single-cell level according to DnaN dynamics (to reduce cell-to-cell variability). Orientation was performed by identifying the cell pole closest to the initially formed replisome. Single-cell time series were aligned in time with the time-shift τ that maximized the cross-correlation

$$\langle (X_t - \langle X \rangle)(Y_{t+\tau} - \langle Y \rangle) \rangle / \sigma_X \sigma_Y$$

over all times t, where X is a time series of DnaN signals selected to be a seed for alignment, and Y is the DnaN time series to be aligned, X_t is a single-time column from X, $\langle X \rangle$ is the mean value of X, and σ_X is the standard deviation of X. The organization factor of a computationally synchronized signal was calculated after additional normalization: polar regions were excluded, the signal was normalized by the area of the mesh segment that it was measured under to obtain signal concentration, C, along the cell length, and C was normalized by setting its integral to 1.

The organization factor of a single signal was then calculated as

$$-\log_2 {}^{1}\!/_{\ell} + \sum C \log_2 C$$

where ℓ is the length of C.

The related code is available in ComputerCodeEV1C

Phylogenetic tree construction

NCBI-retrieved sequences of GapR protein homologs were selected based on representative α-proteobacteria 16S rDNA phylogeny trees (Georgiades et al., 2011; Williams et al., 2007) and complemented with protein sequences of homologs found in other bacterial phyla, α-proteobacteria-related phages, archea and eukarya. Protein sequence alignment was done with MUSCLE (Edgar, 2004) using default parameters. The phylogenetic tree of DUF2312 was made using Genious version 8.1.5 (Kearse et al., 2012) with the Jukes-Cantor genetic distance method and CCNA_03907 (a protein with the highest structural similarity to GapR homologs but not part of the DUF2312 family) as the outgroup. Virus labels include both the viral names and the host species.

194 **Table S1. Strains and plasmids used in this study**

Name	Relevant genotype or description	Reference or source
***C. crescentus* strains**		
CJW1407	CB15N Δ*tipN*	(Lam et al., 2006)
CJW1550	CB15N *vanA*::pNJH17 (*ftsZ-mcherry*)	(Aaron et al., 2007)
CJW2053	CB15N Δ*tipN*::pHL231kbTipNGFP	Whitman Schofield, unpublished
CJW3611	CB15N *tipN*::pCFPC4-tipN'	Whitman Schofield, unpublished
CJW4678	CB15N *dnaN*::pCHYC1-dnaN'	Geraldine Laloux, unpublished
CJW4681	CB15N *dnaN*::pCFPC1-dnaN'	G. Laloux, unpublished
CJW5534	CB15N *gapR*::*gapR-venus*	This work
CJW5535	CB15N *gapR*::*gapR-venus vanA*::pVCFPC2-ftsZ	This work
CJW5537	CB15N *gapR*::*gapR-venus dnaN*::pCHYC1-dnaN'	This work
CJW5594	CB15N *gapR*::*gapR-venus dnaN*::pCFPC1-dnaN' *vanA*::pNJH17	This work
CJW5744	CB15N *xylX*::pXVENC4-gapRp-gapR *dnaN*::pCHYC1-dnaN'	This work
CJW5747	CB15N *ΔgapR*::oxy	This work
CJW5753	CB15N *bla6 rsaA2* pGZ2 *xylX*::pXVENC4-gapRp-gapR	This work
CJW5775	CB15N *bla6 rsaA2* pGZ2 *xylX*:: pXVENC4-gapRp-gapR *dnaN*::pCFPC1-dnaN'	This work
CJW5776	CB15N *xylX*::pXVENC4-gapRp-gapR	This work
CJW5777	CB15N *ΔgapR*::oxy *xylX*::pXVENC4-gapRp-gapR	This work
CJW5781	CB15N *xylX*:: pXCHYC4-gapRp-gapR	This work
CJW5789	CB15N / pRXMCS2	This work
CJW5791	CB15N / pRMCS2-gapRp-gapR	This work
CJW5795	CB15 *divD308*(Ts)::pDW110(parEp), *divE309*(Ts) *xylX*::pVENC4-gapRp-gapR	This work
CJW5796	CB15N *xylX*::pXVENC4	This work

CJW5800	CB15N *xylX*::pXVENC4-PgapR-gapR *dnaN*::pCHYC1-dnaN' *tipN*::pCFPC2-tipN'	This work
CJW5806	CB15N *hu2*::pCHYC2-hu2'	This work
CJW5808	CB15N *xylX*::pXVENC4-PgapR-gapR *dnaN*::pCHYC1-dnaN' *ftsZ*::pBJM1	This work
CJW5810	CB15N *xylX*:: pXCHYC4-gapRp-gapR Δ*tipN*::pHL231kbTipNGFP	This work
CJW5816	CB15N *ΔCCNA_03907*::Ω	This work
CJW5825	CB15N *bla6 rsaA2* pGZ2 *xylX*:: pXVENC4-gapRp-gapR *tipN*::pCFPC1-tipN'	This work
CJW5836	CB15N *xylX*::pXVENC4-gapRp-gapR *dnaN*::pCFPC1-dnaN'	This work
CJW5932	CB15N *gapR*::gapR-venus *tipN*::pCFPC4-tipN' *dnaN*::pCHYC1-dnaN'end	This work
CJW5960	CB15N *hu2*::pCHYC2-hu2' *tipN*::pCFPC1-tipN'	This work
CJW5969	CB15N *hu2*::pCHYC2-hu2' *dnaN*::pCFPC1-dnaNend	This work
EG56	CB15N *vanA*::pVCFPC1-ftsZ	(Goley et al., 2011)
LS1	CB15N *bla6 rsaA2* pGZ2 integrant	(Zweiger et al., 1994)
NA1000	Synchronizable variant of wild-type CB15, also named NA1000 or CB15N	(Evinger and Agabian, 1977)
ML743	Δ*recA*	(Modell et al., 2014)
ML2091	$lexA_{K203A}$	(Modell et al., 2014)
ML2118	CB15N *Δsmc*::km	(Le et al., 2013)
ML2120	CB15N *Δhup1*::sp *Δhup2*::oxy	(Le et al., 2013)
PC6340	CB15 *divD308*(Ts)::pDW110(parEp), *divE309*(Ts). Carrying temperature-sensitive (Ts) mutations in *ftsA* and *parE*	(Ward and Newton, 1997)
YB1585	CB15N *ftsZ*::pBJM1	(Wang et al., 2001)
***E. coli* strains**		
MG1655	K-12 derivative. F-, λ^- -, *rph-1*	(Blattner et al., 1997)
BL21(DE3)	F-, *lon-11*, *Δ(ompT-nfrA)885*, *Δ(galM-*	(Wood, 1966)

	ybhJ)884, *λDE3 [lacI, lacUV5-T7 gene 1, ind1, sam7, nin5]*, *Δ46*, *[mal$^+$]$_{K-12}$*(λ^S), *hsdS10.* Protein expression strain	
DH5α	F-, *Δ(argF-lac)169*, φ80d*lacZ58*(M15), *ΔphoA8*, *glnX44*(AS), *λ$^-$*, *deoR481*, *rfbC1*, *gyrA96*(NalR), *recA1*, *endA1*, *thiE1*, *hsdR17*. Cloning strain	Invitrogen
S17-1	*recA pro hsdR* RP4-2-Tc::Mu-Km::Tn7, used for conjugation	(Simon R et al., 1984)
SM10	F-, λ$^-$, *thr-1, leuB6, lacY1, supE44, rfbD1, thi-1, tonA21, recA* RP4 derivative integrated into the chromosome, Tet::Mu. Used for conjugation.	MRK Alley, unpublished
CJW5794	MG1655/ pBAD33-gapR-sfGFP	This work
CJW5785	BL21 (DE)/ pET24dHT-GapR	This work
***Plasmids*[&]**		
pBAD33	Replicative vector with *ori* p15A origin and *cat* gene (Cm^r) for expression of proteins under control or arabinose promoter in *E.coli*	(Guzman et al., 1995)
pBAD33-gapR-sfGFP	pBAD33 derivative for expression of *gapR-sfgfp* in *E. coli,* Cm^r	This work
pBOR	pBluescript with Ω cassette from pHP45Ω cloned at EcoRI site, Sp^r	C. Stevens, unpublished
pCFPC1 (pMT622)	Non-replicative plasmid in *C. crescentus,* used for generating a C-terminus CFP protein fusion expressed from chromosomal loci, Sp^r	(Thanbichler et al., 2007)
pCFPC1-dnaN'	Plasmid for generating a C-terminus CFP protein fusion of DnaN expressed from the *dnaN* chromosomal locus, Sp^r	G. Laloux, unpublished
pCFPC1-tipN'	Plasmid for generating a C-terminus CFP protein fusion of TipN expressed from the *tipN* chromosomal locus, Sp^r	This work
pCFPC2 (pMT664)	Non-replicative plasmid in *C. crescentus,* used for generating a C-terminus CFP protein fusion expressed from chromosomal loci, Km^r	(Thanbichler et al., 2007)
pCFPC2-tipN'	Plasmid for generating a C-terminus CFP protein fusion of TipN expressed from the *tipN*	W. Schofield, unpublished

	chromosomal locus, Km^r	
pCHYC1 (pMT625)	Non-replicative plasmid in *C. crescentus,* used for generating a C-terminus mCherry protein fusion expressed from chromosomal loci, Sp^r	(Thanbichler et al., 2007)
pCHYC1-dnaN'	Plasmid for generating a C-terminus mCherry protein fusion of DnaN expressed from the *dnaN* chromosomal locus, Sp^r	G. Laloux, unpublished
pCHYC2	Non-replicative plasmid in *C. crescentus,* used for generating a C-terminus mCherry protein fusion expressed from chromosomal loci, Km^r	(Thanbichler et al., 2007)
pCHYC2-Hu2	Plasmid for generating a C-terminus mCherry protein fusion of *hu2* expressed from the *hu2* chromosomal locus, Km^r	This work
pET24dHTcreSΔH	Derivative of pET24dHT (gift of N. Foeger, Heidelberg, Germany to Matthew T. Cabeen). Empty plasmid was originally engineered from pET24d (Novagen) to have a His-tag and a TEV protease cleavage site upstream the NdeI site for cloning, Km^r	Matthew T. Cabeen, unpublished
pET24dHT-GapR	Plasmid for overproduction and purification of 6xHis-GapR, Km^r	This work
pHL23	Cloning vector, Km^r	(Lam et al., 2006)
pHL231kbTipNGFP	A fragment containing *tipN-gfp* was released from pKStipN-GFP by digestion with Not1 and included into pHL23 carrying TipN and ~1Kb upstream the *tipN* locus.	W. Schofield, unpublished
pIDTcc3319	DNA sequence of *gapR* gene that has been codon-optimized for *E. coli* was cloned into a plasmid from IDT (Integrated DNA Technologies, Coralville IA), Km^r	This work
pKStipN-GFP	pBluescript carrying *tipN-gfp*	(Lam et al., 2006)
pNPTS138	*mobRP4*$^+$ *sacB* ColE1 *ori,* Km^r	M.R. Alley, unpublished
pNPTS138UPΩDWccna_03907	Integrative vector for in-frame deletion of *CCNA_03907* and replacement with spectinomycin resistance (Ω) cassette, Km^r, Sp^r	This work

pNPTS138UPOxyDWgapR	Integrative vector for in-frame deletion of *gapR* and replacement with oxytetracycline (Oxy^r) resistance cassette, Km^r,	This work
pNPTS138-gapR-Venus	Integrative vector for replacement of *gapR* for a *gapR-Venus* fusion at *gapR* gene locus, Km^r.	This work
pRXMCS2 (pMT687)	Replicative plasmid in *C. crescentus*, used for inducible expression of genes from a low-copy number plasmid, Km^r	(Thanbichler et al., 2007)
pRMCS2-gapRp-gapR	pRXMCS2 derivative. Vector for *gapR* expression under the control of its own promoter in *C. crescentus*, Km^r	This work
pTOPO2.1	Cloning vector, Ap^r, Km^r	Thermo Fisher Scientific
pXCFPC5 (pMT605)	Non-replicative plasmid in *C. crescentus,* used for generating a C-terminus CFP protein fusion expressed at the *xylX* locus, Tet^r	(Thanbichler et al., 2007)
pXCHYC4 (pMT617)	Non-replicative plasmid in *C. crescentus,* used for generating a C-terminus Venus protein fusion expressed at the *xylX* locus, Gn^r	(Thanbichler et al., 2007)
pXCHYC4-gapRp-gapR	Plasmid for generating a C-terminus mCherry protein fusion of GapR expressed under the control of *gapR* promoter from the *xylX* locus, Gn^r	This work
pXVENC4 (pMT616)	Non-replicative plasmid in *C. crescentus,* used for generating a C-terminus Venus protein fusion expressed at the *xylX* locus, Gn^r	(Thanbichler et al., 2007)
pXVENC4-gapRp-gapR	Plasmid for generating a C-terminus Venus protein fusion of GapR expressed under the control of *gapR* promoter from the *xylX* locus, Gn^r	This work

[&]Vector resistance: Ap^r, Ampicillin, Cm^r, Chloramphenicol, Gn^r, Gentamicin, Km^r, Kanamycin resistance, Oxy^r, oxytetracycline, Sp^r, Spectinomycin.

199 **Table S2. Construction of strains and plasmids used in this study**

Strain or plasmid	Construction method
Strain	
CJW2053	Transformation of pHL231kbTipNGFP into CJW1407.
CJW3611	Transformation of pCFPC-4TipN into CB15N.
CJW4678	Transformation of pCHYC1-dnaN' into CB15N.
CJW5534	A strain carrying a *gapR-venus* as the only copy was created using a two-step gene disruption method and sucrose selection as described previously (Gay et al., 1985). Clones were verified by sensitivity to kanamycin. Acquisition of *gapR-venus* was verified by PCR amplification with oligomers cjw2099-cjw2102 and fluorescence microscopy.
CJW5535	An UV-inactivated ΦCR30 phage lysate carrying *vanA*::ftsZ-CFP was obtained from strain EG56 and used for transduction into CJW5534.
CJW5537	An UV-inactivated ΦCR30 phage lysate carrying *dnaN*::pCFPC1-dnaN' was obtained from strain CJW4681 and used for transduction into CJW5534.
CJW5594	An UV-inactivated ΦCR30 phage lysate carrying *vanA*::pNJH17 was obtained from strain CJW1550 and used for transduction into CJW5537.
CJW5744	Plasmid pXVENC4-gapRp-gapR was transformed into the S17-1 strain and introduced into CJW4678 by conjugation with selection of gentamicin and nalidixic acid resistance.
CJW5747	An UV-inactivated ΦCR30 phage lysate carrying Δ*gapR*::oxy was obtained from CJW5777. Δ*gapR*::oxy was transduced into CB15N by incubation of 50 to 100 µL of UV-radiated phage lysate with 400 µL of recipient cells. Transductants were selected on PYE agar plates containing oxytetracycline (oxy), and incubated at room temperature for 5 to 10 days. Acquisition of the Δ*gapR*::oxy deletion was verified by PCR amplification with oligomers cjw2099-cjw2102. Verification of additional mutations was performed by whole genome sequencing and analyzed against CB15N using breseq software (Deatherage and Barrick, 2014).
CJW5753	Plasmid pXVENC4-gapRp-gapR was transformed into the S17-1 strain and introduced into LS1 by conjugation with selection of gentamicin and nalidixic acid resistance.
CJW5775	An UV-inactivated ΦCR30 phage lysate carrying *dnaN*::pCFPC1-dnaN'

	was obtained from strain CJW4681 and used for transduction into CJW5753
CJW5776	Transformation of pXVENC4-gapRp-gapR into CB15N.
CJW5777	A strain carrying a deletion of *gapR* and carrying an oxytetracycline resistance cassette in its place was created using a two-step gene disruption method and sucrose selection, as described previously (Gay et al., 1985). Clones were selected by sensitivity for kanamycin and resistance to oxytetracycline. Acquisition of the Δ*gapR*::*oxy* was verified by PCR amplification with oligomers cjw2099-cjw2102.
CJW5789	Transformation of pRXMCS2 into CB15N
CJW5791	Transformation of pRMCS2-gapRp-gapR into CB15N
CJW5794	Transformation of pBAD33-gapR-sfGFP into MG1655
CJW5795	Plasmid pXVENC4-gapRp-gapR was transformed into the S17-1 strain and introduced into strain PC6340 by conjugation with selection of gentamicin, nalidixic acid resistance and growth at room temperature.
CJW5796	Transformation of pXVENC4 into CB15N
CJW5800	Plasmid pCFPC2-tipN' was transformed into the S17-1 strain, and introduced into CJW5744 by conjugation with selection of kanamycin and nalidixic acid resistance.
CJW5806	Transformation of pCHYC2-Hu2 into CB15N
CJW5808	An UV-inactivated ΦCR30 phage lysate carrying *ftsZ*::pBJM1 was obtained from using strain YB1585. *ftsZ*::pBJM1 was transduced into CB15N and transductants were selected on PYE kanamycin plate containing xylose 0.3% at 30°C.
CJW5810	Transformatin of pXCHYC4-gapRp-gapR into CJW2053.
CJW5816	Plasmid CJW5817 was electroporated into CB15N. Deletion of *ccna_03907* was made using a gene disruption method and sucrose selection, as described previously (Gay et al., 1985). Clones were selected by sensitivity for kanamycin and resistance to spectinomycin and verified by PCR using oligomers cjw2618-cjw2619.
CJW5825	Plasmid pCFPC1-tipN' was transformed into the SM10 strain and introduced into CJW5753 by selection of spectinomycin and nalidixic acid resistance.
CJW5836	An UV-inactivated ΦCR30 phage lysate carrying *dnaN*::pCFPC1-dnaN' was obtained from strain CJW4681 and used for transduction into CJW5776.

CJW5932	An UV-inactivated ΦCR30 phage lysate carrying *tipN*::pCFPC4-tipN' was obtained from strain CJW3611 and used for transduction into CJW5534. Subsequently, the *dnaN*::pCHYC1-dnaN' fusion was introduced in the resulting strain by transduction using an UV-inactivated ΦCR30 phage lysate from strain CJW4678.
CJW5960	Plasmid pCFPC1-tipN' was transformed into the SM10 strain, and introduced into CJW5806 by conjugation with selection of spectinomycin and nalidixic acid resistance.
CJW5969	An UV-inactivated ΦCR30 phage lysate carrying *dnaN*::pCHYC1-dnaNend' was obtained from strain CJW4681 and used for transduction into strain CJW5824
*Plasmid**	
pBAD33-gapR-sfGFP	The *gapR* gene was PCR amplified using oligomers cjw2325-cjw2326 and the superfolderGFP (sfGFP) was PCR amplified with oligomers cjw2327-cjw2328 from *E. coli* codon-optimized templates. Both fragments were introduced into a previously digested pBAD33 via Gibson* assembly at the NdeI and HindIII restriction sites. Incorporation of the fragment into this region of the plasmid was verified by sequencing.
pCFPC1-dnaN'	The 3' end of *dnaN* was amplified using oligomers cjw1822-cjw1823 from a CB15N genomic DNA template. PCR product was digested with KpnI and NdeI, and ligated into pCFPC1 previously digested with the same restriction enzymes. Plasmid was verified by sequencing.
pCFPC1-tipN'	The 3' end of *tipN* fragment was released from plasmid pCFPC2-tipN' by digestion with SalI and KpnI into pMT622 previously digested with the same restriction enzymes.
pCFPC2-tipN'	The 3' end of *tipN* was amplified using oligomers cjw1205-cjw1206 from a CB15N genomic DNA template, and introduced in a pTOPO2.1 vector. The resulting plasmid was verified by sequencing. A *tipN* fragment was released with SalI and KpnI from the plasmid, and ligated into pCFPC2 previously digested with the same restriction enzymes.
pCFPC4-tipN'	The 3' end of *tipN* was amplified using oligomers cjw1205-cjw1206 from a CB15N genomic DNA template, and introduced in a pTOPO2.1 vector. The resulting plasmid was verified by sequencing. A *tipN* fragment was released with SalI and KpnI from the plasmid, and ligated into pCFPC4 previously digested with the same restriction enzymes.

pCHYC1-dnaN'	The 3' end of *dnaN* was amplified using oligomers cjw1822-cjw1823 from a CB15N genomic DNA template. PCR product was digested with KpnI and NdeI, and ligated into pCHYC1 previously digested with the same restriction enzymes. Plasmid was verified by sequencing.
pCHYC2-Hu2'	The 3' end of *hu2* was amplified using oligomers cjw2768-cjw2769 from a CB15N genomic DNA template. PCR product was digested with KpnI and NdeI, and ligated into pCHYC2 previously digested with the same restriction enzymes. Plasmid was verified by sequencing.
pET24dHT-GapR	The *gapR* gene was PCR amplified with oligomers cjw2329-cjw2330 from plasmid pIDTcc3319 used as template. The PCR product was digested with NdeI and HindIII and ligated into pET24dHTcreSDH previously digested with the same restriction enzymes and extracted from gel. Clones were verified by sequencing.
pNPTS138UPΩDW ccna_03907	The 1 Kb upstream of the *CCNA_03907* region (UP) including the beginning of the gene was PCR amplified with oligomers cjw2614-cjw2651 and the 1 Kb downstream region of *CCNA_03907* starting at the very end of the gene (DW) was also PCR amplified using oligomers cjw2652-cjw2653. CB15N genomic DNA was the template. The PCR products and the spectinomycin (Ω) cassette (obtained by amplification from pBOR with oligomers cjw2746-cjw2747) were introduced into a pNPTS138 plasmid via Gibson* assembly at the HindIII and NheI restriction sites. Incorporation of the fragment into this region of the plasmid was verified by sequencing.
pNPTS138UPoxyDWgapR	The 1 Kb upstream of the *gapR* region (UP) including the beginning of the gene was PCR amplified with oligomers cjw2099-cjw2173 and the 1 Kb downstream region of *gapR* starting at the very end of the gene (DW) was also PCR amplified using oligomers cjw2102-cjw2174. CB15N genomic DNA was used as a template. The PCR products and the oxytetracycline resistance cassette (obtained by amplification from pXCFPC5 with oligomers cjw2748 and cjw2749) were introduced into a pNPTS138 plasmid via Gibson* assembly at the HindIII and NheI restriction sites. Incorporation of the fragment into this region of the plasmid was verified by sequencing.
pNPTS138-gapR-Venus	The 1 Kb upstream of the *gapR* region (UP) including the very beginning of the gene was PCR amplified with oligomers cjw2099-cjw2179 and the 1 Kb downstream region of *gapR* starting at the very end of the gene (DW) was also PCR amplified using oligomers

	cjw2102-cjw2151. CB15N genomic DNA was the template. The *gapR-venus* gene fusion was PCR amplified using genomic DNA from strain CJW5776 with oligomers cjw2148-cjw2149. These PCR products were introduced into a pNPTS138 via Gibson* assembly at the HindIII and NheI restriction sites. Incorporation of the fragment into this region of the plasmid was verified by sequencing.
pRMCS2-gapRp-gapR	A fragment including the region between the promoter of *gapR* (*gapRp*) and the end of the *gapR* gene was PCR amplified with oligomers cjw2424-cjw2425 from a CB15N genomic DNA template. The amplified fragment was introduced via Gibson* assembly protocol into a previously PCR amplified pMT687 using oligomers cjw2426-cjw2427 (to remove the xylX promoter (*xylXp*). Incorporation of the fragment into the region downstream the NcoI restriction site of *xylXp* and upsteam the NheI restriction site of the plasmid was verified by sequencing.
pXVENC4-gapRp-gapR	A fragment including the region between the *gapR* promoter and the end of the *gapR* gene was PCR amplified with oligomers cjw2105-cjw2106 from a CB15N genomic DNA template. The amplified fragment was introduced via Gibson* assembly protocol into a previously PCR amplified pXVENC4 using oligomers cjw2033-cjw1863 (to remove the *xylX* promoter). Incorporation of the fragment into the region downstream the NcoI restriction site of the *xylX promoter* and upsteam the NheI restriction site of the plasmid was verified by sequencing.
pXCHYC4-gapRp-gapR	A fragment including the region between the *gapR* promoter and the end of the *gapR* gene was PCR amplified with oligomers cjw2105-cjw2106 from a CB15N genomic DNA template. The amplified fragment was introduced via Gibson* assembly protocol into a previously PCR amplified pXCHYC4 using oligomers cjw2033-cjw1863 (to remove the *xylX* promoter). Incorporation of the fragment into the region downstream the NcoI restriction site of the *xylX promoter* and upsteam the NheI restriction site of the plasmid was verified by sequencing.

*Procedure for the Gibson assembly protocol was adapted from Gibson DG et al (Gibson et al., 2009).

Table S3. List of oligonucleotides used in this study

Oligonucleotide	Sequence
Cloning	
cjw1205	CCCCCATATGAAGCCTAAGAAGCGCCAACC
cjw1206	CCCCGGTACCGGCCAGATCGCCGCTCGCCG
cjw1221	TCCCCGCGGGACCTTCGGTCTTCCACAAA
cjw1222	AGACTGCGACAGGGTCTCC
cjw1822	CCCCCATATGCCGAGGGCGCGGTCGGCATC
cjw1822	CCCCCATATGCCGAGGGCGCGGTCGGCATC
cjw1823	AAAAGGTACCGACCCGCAGCGGCATCAGCAC
cjw1823	AAAAGGTACCGACCCGCAGCGGCATCAGCAC
cjw1863	GGTACCTTAAGATCTCGAGC
cjw2033	CCATGGCCCGCGCCCAGTTCCGCCT
cjw2099	GTGCAATTGAAGCCGGCTGGCGCCAAGCTTCGGGTGAAGTTCCCGCCCTGCGCCG
cjw2100	TCCACTAGTTCTAGAGCGGCCATGGGGGCGTCTCGCGAAAGGCAG
cjw2101	TTGCTCAATCAATCACCGGATAGGTTTTTCAGCGTGCGTCGGCGC
cjw2102	CATCCGGAGACGCGTCACGGCCGAAGCTAGCGATAGGCGGACTCCACCGGTGATCC
cjw2103	ATCACTTTACCGACCCGGCC
cjw2104	AAACTCACCCTCCCATTCGG
cjw2105	GCGGAACTGGGCGCGGGCCATGGGCGAGGATCGGTCGGCCAGACGCGG
cjw2106	GCTCGAGATCTTAAGGTACCGATCTCGCCGATCGCCGACAGATAG
cjw2148	CTGCCTTTCGCGAGACGCCCCCATG
cjw2149	CACGCGCCGACGCACGCTGAAAAACTTACTTGTACAGCTCGTCCATGCCG
cjw2151	GTTTTTCAGCGTGCGTCGGCGCGTG
cjw2173	ATTCTTGAAGACGAAAGGGCCTCGCATGGGGGCGTCTCGCGAAAGGCAG
cjw2174	GTCCAAGCCTCACGGCCGCGCTCGTAGGTTTTTCAGCGTGCGTCGGCGC
cjw2179	CATGGGGGCGTCTCGCGAAAGGCAG
cjw2325	GCTAGCGAATTCGAGCTCGGTACCGAAGGAGGGCCATATGGCCGACGACGCCATTCCC
cjw2326	GGTGGCCGACCGGTGACGCGTAATTTCACCAATTGCCGACAGATAC
cjw2327	ACGCGTCACCGGTCGGCCACCATGTCAAAAGGCGAAGAACTTTTT
cjw2328	CTCATCCGCCAAAACAGCCAAGCTTTTATTTATACAATTCATCCATTCC
cjw2329	GGAATTCCATATGGCGGACGACGCAATTCCGCATA
cjw2330	CCAAGCTTCTAAATTTCACCAATTGCCGACAG
cjw2424	CTGGGCCTTTCGTTTTATCTGTTGTTTGTCGGCGAGGATCGGTCGGCCAGACGCGG
cjw2425	GAACTAGTGGATCCCCCGGGCTGCAGCTAGCCTAGATCTCGCCGATCGCCGACAGA
cjw2426	CGACAAACAACAGATAAAACGAAAGGCCCAG
cjw2427	GCTAGCTGCAGCCCGGGGGATCCACTAGTTC

cjw2614	GTGCAATTGAAGCCGGCTGGCGCCAAGCTTGTCGGCAATGTCATCGTGCGCTGGG
cjw2618	CGACGTTAAGGTGCTCAAGAAGGTGG
cjw2619	CCTAACGCAGTTCGCGGAACGGCAG
cjw2651	CCAGCCTGCGCGAGCAGGGGAATTGGGTCGGGACTTATCCCGCACGCCACGCGCC
cjw2652	CTAGCGAGGGCTTTACTAAGCTGATACCGACCTGCGATTTCCGGCAGGTAGGATT
cjw2653	GAGACGCGTCACGGCCGAAGCTAGCTGCCGGCCACATGAGCGAGGTCGCGCGGCG
cjw2736	GTGCCTAATGAGTGAGCTAAC
cjw2737	GTGGAATTGTGAGCGGATAAC
cjw2738	GTTAGCTCACTCATTAGGCACGAATTCTAAAGATCTTTGACAGCTAG
cjw2739	GTTATCCGCTCACAATTCCACGCAGCGAGTCAGTGAGCG
cjw2746	CAATTCCCCTGCTCGCGCAGGCTGG
cjw2747	ATCAGCTTAGTAAAGCCCTCGCTAG
cjw2748	CGAGGCCCTTTCGTCTTCAAG
cjw2749	CGAGCGCGGCCGTGAGGCTT
cjw2768	GAGACGTCCAATTGCATATGAACGTTTCCGATCTGGTCGACGCCG
cjw2769	GCTCGAGATCTTAAGGTACCGCCGTTGACGGCGTCCTTCAGTTGC
EMSA assay	
cjw2750	ATTAAGTGCAGTCGGCGAAATTGATCGTGTTTTCGGGGGTGAGCAAGTCG
cjw2751	CGACTTGCTCACCCCCGAAAACACGATCAATTTCGCCGACTGCACTTAAT

Appendix References

Aaron, M., Charbon, G., Lam, H., Schwarz, H., Vollmer, W., and Jacobs-Wagner, C. (2007). The tubulin homologue FtsZ contributes to cell elongation by guiding cell wall precursor synthesis in Caulobacter crescentus. Mol Microbiol *64*, 938-952.

Blattner, F.R., Plunkett, G., 3rd, Bloch, C.A., Perna, N.T., Burland, V., Riley, M., Collado-Vides, J., Glasner, J.D., Rode, C.K., Mayhew, G.F.*, et al.* (1997). The complete genome sequence of Escherichia coli K-12. Science *277*, 1453-1462.

Deatherage, D.E., and Barrick, J.E. (2014). Identification of mutations in laboratory-evolved microbes from next-generation sequencing data using breseq. Methods Mol Biol *1151*, 165-188.

Dobin, A., Davis, C.A., Schlesinger, F., Drenkow, J., Zaleski, C., Jha, S., Batut, P., Chaisson, M., and Gingeras, T.R. (2013). STAR: ultrafast universal RNA-seq aligner. Bioinformatics *29*, 15-21.

Edgar, R.C. (2004). MUSCLE: multiple sequence alignment with high accuracy and high throughput. Nucleic Acids Res *32*, 1792-1797.

Evinger, M., and Agabian, N. (1977). Envelope-associated nucleoid from Caulobacter crescentus stalked and swarmer cells. Journal of bacteriology *132*, 294-301.

Figge, R.M., Divakaruni, A.V., and Gober, J.W. (2004). MreB, the cell shape-determining bacterial actin homologue, co-ordinates cell wall morphogenesis in Caulobacter crescentus. Mol Microbiol *51*, 1321-1332.

Gay, P., Le Coq, D., Steinmetz, M., Berkelman, T., and Kado, C.I. (1985). Positive selection procedure for entrapment of insertion sequence elements in gram-negative bacteria. Journal of bacteriology *164*, 918-921.

Georgiades, K., Madoui, M.A., Le, P., Robert, C., and Raoult, D. (2011). Phylogenomic analysis of Odyssella thessalonicensis fortifies the common origin of Rickettsiales, Pelagibacter ubique and Reclimonas americana mitochondrion. PloS one *6*, e24857.

Gibson, D.G., Young, L., Chuang, R.Y., Venter, J.C., Hutchison, C.A., 3rd, and Smith, H.O. (2009). Enzymatic assembly of DNA molecules up to several hundred kilobases. Nat Methods *6*, 343-345.

Goley, E.D., Yeh, Y.C., Hong, S.H., Fero, M.J., Abeliuk, E., McAdams, H.H., and Shapiro, L. (2011). Assembly of the Caulobacter cell division machine. Mol Microbiol *80*, 1680-1698.

Guzman, L.M., Belin, D., Carson, M.J., and Beckwith, J. (1995). Tight regulation, modulation, and high-level expression by vectors containing the arabinose PBAD promoter. Journal of bacteriology *177*, 4121-4130.

Kearse, M., Moir, R., Wilson, A., Stones-Havas, S., Cheung, M., Sturrock, S., Buxton, S., Cooper, A., Markowitz, S., Duran, C.*, et al.* (2012). Geneious Basic: an integrated and extendable desktop software platform for the organization and analysis of sequence data. Bioinformatics *28*, 1647-1649.

Krzywinski, M., Schein, J., Birol, I., Connors, J., Gascoyne, R., Horsman, D., Jones, S.J., and Marra, M.A. (2009). Circos: an information aesthetic for comparative genomics. Genome Res *19*, 1639-1645.

Lam, H., Schofield, W.B., and Jacobs-Wagner, C. (2006). A landmark protein essential for establishing and perpetuating the polarity of a bacterial cell. Cell *124*, 1011-1023.

Le, T.B., Imakaev, M.V., Mirny, L.A., and Laub, M.T. (2013). High-resolution mapping of the spatial organization of a bacterial chromosome. Science *342*, 731-734.

Li, H., and Durbin, R. (2009). Fast and accurate short read alignment with Burrows-Wheeler transform. Bioinformatics *25*, 1754-1760.

Liao, Y., Smyth, G.K., and Shi, W. (2014). featureCounts: an efficient general purpose program for assigning sequence reads to genomic features. Bioinformatics *30*, 923-930.

Love, M.I., Huber, W., and Anders, S. (2014). Moderated estimation of fold change and dispersion for RNA-seq data with DESeq2. Genome Biol *15*, 550.

Machanick, P., and Bailey, T.L. (2011). MEME-ChIP: motif analysis of large DNA datasets. Bioinformatics *27*, 1696-1697.

Modell, J.W., Kambara, T.K., Perchuk, B.S., and Laub, M.T. (2014). A DNA damage-induced, SOS-independent checkpoint regulates cell division in Caulobacter crescentus. PLoS Biol *12*, e1001977.

Quinlan, A.R., and Hall, I.M. (2010). The Bedtools manual.

Quon, K.C., Marczynski, G.T., and Shapiro, L. (1996). Cell cycle control by an essential bacterial two-component signal transduction protein. Cell *84*, 83-93.

Simon R, Priefer U, and A, P. (1984). A broad host range mobilization system for invivo genetic-engineering - transposon mutagenesis in gram-negative bacteria. Bio-Technol *1*, 784-791.

Sun, H., Yuan, Y., Wu, Y., Liu, H., Liu, J.S., and Xie, H. (2010). Tmod: toolbox of motif discovery. Bioinformatics *26*, 405-407.

Thanbichler, M., Iniesta, A.A., and Shapiro, L. (2007). A comprehensive set of plasmids for vanillate- and xylose-inducible gene expression in Caulobacter crescentus. Nucleic Acids Res *35*, e137.

Wang, Y., Jones, B.D., and Brun, Y.V. (2001). A set of ftsZ mutants blocked at different stages of cell division in Caulobacter. Mol Microbiol *40*, 347-360.

Ward, D., and Newton, A. (1997). Requirement of topoisomerase IV parC and parE genes for cell cycle progression and developmental regulation in Caulobacter crescentus. Mol Microbiol *26*, 897-910.

Williams, K.P., Sobral, B.W., and Dickerman, A.W. (2007). A robust species tree for the alphaproteobacteria. Journal of bacteriology *189*, 4578-4586.

Wood, W.B. (1966). Host specificity of DNA produced by Escherichia coli: bacterial mutations affecting the restriction and modification of DNA. J Mol Biol *16*, 118-133.

Zhang, Y., Liu, T., Meyer, C.A., Eeckhoute, J., Johnson, D.S., Bernstein, B.E., Nusbaum, C., Myers, R.M., Brown, M., Li, W.*, et al.* (2008). Model-based analysis of ChIP-Seq (MACS). Genome Biol *9*, R137.

Zweiger, G., Marczynski, G., and Shapiro, L. (1994). A Caulobacter DNA methyltransferase that functions only in the predivisional cell. J Mol Biol *235*, 472-485.